FINNISH METEOROLOGICAL INSTITUTE
CONTRIBUTIONS

No. 59

ON THE BEHAVIOUR OF SOME PHYSICAL PARAMETERIZATION METHODS IN HIGH-RESOLUTION NUMERICAL WEATHER PREDICTION MODELS

Sami Niemelä

Department of Physical Sciences
Faculty of Science
University of Helsinki
Helsinki, Finland

ACADEMIC DISSERTATION in meteorology

To be presented, with the permission of the Faculty of Science of the University of Helsinki, for public critisism in Auditorium Physicum E204 (Gustaf Hällströmin katu 2) on January 26th, 2007, at 12 o'clock noon.

Finnish Meteorological Institute
Helsinki, 2006

ISBN 951-697-620-4 (paperback)
ISBN 952-10-3613-3 (pdf)
ISSN 0782-6117

Yliopistopaino
Helsinki, 2006

FINNISH METEOROLOGICAL INSTITUTE

Published by Finnish Meteorological Institute

P.O. Box 503
FIN-00101 Helsinki, Finland

Series title, number and report code of publication
Finnish Meteorological Institute
Contributions 59, FMI-CONT-59

Date
December 2006

Authors
Sami Niemelä

Name of project

Commissioned by

Title
On the behaviour of some physical parameterization methods in high-resolution numerical weather prediction models

Abstract

Modern-day weather forecasting is highly dependent on Numerical Weather Prediction (NWP) models as the main data source. The evolving state of the atmosphere with time can be numerically predicted by solving a set of hydrodynamic equations, if the initial state is known. However, such a modelling approach always contains approximations that by and large depend on the purpose of use and resolution of the models. Present-day NWP systems operate with horizontal model resolutions in the range from about 40 km to 10 km. Recently, the aim has been to reach operationally to scales of 1 – 4 km. This requires less approximations in the model equations, more complex treatment of physical processes and, furthermore, more computing power. This thesis concentrates on the physical parameterization methods used in high-resolution NWP models. The main emphasis is on the validation of the grid-size-dependent convection parameterization in the High Resolution Limited Area Model (HIRLAM) and on a comprehensive intercomparison of radiative-flux parameterizations. In addition, the problems related to wind prediction near the coastline are addressed with high-resolution meso-scale models.

The grid-size-dependent convection parameterization is clearly beneficial for NWP models operating with a dense grid. Results show that the current convection scheme in HIRLAM is still applicable down to a 5.6 km grid size. However, with further improved model resolution, the tendency of the model to overestimate strong precipitation intensities increases in all the experiment runs.

For the clear-sky longwave radiation parameterization, schemes used in NWP-models provide much better results in comparison with simple empirical schemes. On the other hand, for the shortwave part of the spectrum, the empirical schemes are more competitive for producing fairly accurate surface fluxes. Overall, even the complex radiation parameterization schemes used in NWP-models seem to be slightly too transparent for both long- and shortwave radiation in clear-sky conditions. For cloudy conditions, simple cloud correction functions are tested. In case of longwave radiation, the empirical cloud correction methods provide rather accurate results, whereas for shortwave radiation the benefit is only marginal.

Idealised high-resolution two-dimensional meso-scale model experiments suggest that the reason for the observed formation of the afternoon low level jet (LLJ) over the Gulf of Finland is an inertial oscillation mechanism, when the large-scale flow is from the south-east or west directions. The LLJ is further enhanced by the sea-breeze circulation. A three-dimensional HIRLAM experiment, with a 7.7 km grid size, is able to generate a similar LLJ flow structure as suggested by the 2D-experiments and observations. It is also pointed out that improved model resolution does not necessary lead to better wind forecasts in the statistical sense. In nested systems, the quality of the large-scale host model is really important, especially if the inner meso-scale model domain is small.

Publishing unit
Finnish Meteorological Institute, Meteorological Research Unit

Classification (UDC)
551.509.313.43

Keywords
meso-scale NWP, convection, microphysics, radiation

ISSN and series title
0782-6117 Finnish Meteorological Institute Contributions

ISBN
951-697-620-4 (paperback), 952-10-3613-3 (pdf)

Language
English

Pages
136

Price

Sold by
Finnish Meteorological Institute / Library
P.O. Box 503, FIN-00101 Helsinki, Finland

Note

ILMATIETEEN LAITOS

Julkaisija Ilmatieteen laitos

PL 503, 00101 Helsinki

Julkaisun sarja, numero ja raporttikoodi
Finnish Meteorological Institute
Contributions 59, FMI-CONT-59

Julkaisuaika
Joulukuu 2006

Tekijä(t)
Sami Niemelä

Projektin nimi

Toimeksiantaja

Nimike
Fysikaalisia parametrisointimenetelmiä tarkan erotuskyvyn numeerisissa sääennustusmalleissa.

Tiivistelmä

Nykypäivänä sään ennustaminen perustuu suurelta osin numeerisen sääennustusjärjestelmän tuottamaan aineistoon. Ilmakehän tila voidaan ennalta määrittää ratkaisemalla numeerisesti ilmakehää kuvaava hydrodynaaminen yhtälöryhmä, mikäli alkutila tunnetaan. Tällainen ilmakehämalli sisältää enemmän tai vähemmän yksinkertaistuksia riippuen mallin erotuskyvystä ja käyttötarkoituksesta. Nykyään operatiivisten sääennustusjärjestelmien vaakasuuntainen erotuskyky on n. 10 – 40 km. Lähitulevaisuuden operatiivinen tavoite on saavuttaa 1 – 4 km erotuskyky. Tavoite vaatii malliyhtälöiden sisältämien yksinkertaistuksien vähentämistä, fysikaalisten prosessien monimutkaisempaa kuvaamista sekä enemmän laskentatehoa. Tämä väitöskirja keskittyy tarkan erotuskyvyn sääennustusmallien fysikaalisiin parametrisointimenetelmiin. Päähuomio kohdistuu HIRLAMin (High Resolution Limited Area Model) hilavälistä riippuvan konvektion parametrisoinnin sekä maan pinnalle tulevien säteilyvoiden parametrisointimenetelmien arvioimiseen uealla eri menetelmällä. Väitöskirjassa tarkastellaan lisäksi tuulen ennustamista tarkan resoluution mesoskaalamalleilla rannikon läheisyydessä.

Hilavälistä riippuvasta konvektion parametrisoinnista on selvästi hyötyä tarkan erotuskyvyn sääennustusmalleille. Tulokset osoittavat, että nykyinen HIRLAMin konvektion parametrisointi on vielä käyttökelpoinen 5.6 km hilaväliä käytettäessä. Kun erotuskykyä tarkennetaan tätä paremmaksi, mallin taipumus yliarvioida voimakkaita sateita kasvaa kaikissa tehdyissä kokeissa.

Sääennustusmalleissa käytetyt pitkäaaltoisen säteilyvuon parametrisointimenetelmät tuottavat pilvettömissä tilanteissa selvästi parempia tuloksia kuin yksinkertaiset kokeelliset laskentamenetelmät. Sen sijaan lyhytaaltoisen säteilyvuon laskennassa pilvettömissä tilanteissa myös kokeelliset menetelmät osoittautuvat kilpailukykyisiksi monimutkaisiin parametrisointeihin verrattuna. Sääennustusmalleissa käytettävien säteilyn parametrisointien kuvaama ilmakehä on hieman liian läpinäkyvä sekä pitkä- että lyhytaaltosäteilylle pilvettömissä olosuhteissa. Siitä huolimatta kyseiset menetelmät tuottavat yleisesti parempia tuloksia kuin yksinkertaiset menetelmät. Pilvisissä tilanteissa säteilyvuon laskennassa on testattu yksinkertaisia pilvikorjausmenetelmiä. Kokeelliset pilvikorjausmenetelmät tuottavat pitkäaaltosäteilyn laskennassa melko hyviä tuloksia, kun taas lyhytaaltosäteilyn tapauksessa kyseisistä menetelmistä on vain marginaalisesti hyötyä.

Idealisoitujen kaksiulotteisten mesoskaalan mallikokeiden perusteella voidaan osoittaa, että inertiaalivärähtelymekanismi on pääsyy matalan suihkuvirtauksen muodostumiselle Suomenlahden ylle, kun laajan skaalan tuulen suunta on joko kaakosta tai lännestä. Suihkuvirtaus voimistuu entisestään merituulikiertoliikkeen vaikutuksesta. Kolmiulotteinen HIRLAM-malli 7.7 km hilavälillä muodostaa samankaltaisen matalan suihkuvirtauksen kuin kaksiulotteiset mallikokeet ja havainnot osoittavat. Mallin erotuskyvyn parantaminen ei kuitenkaan välttämättä johda parempiin tuuliennusteisiin. Sisäkkäisissä mallijärjestelmissä laajan skaalan “isäntämallin” tulosten laatu on erittäin merkittävä tekijä myös tarkan erotuskyvyn mallin tulosten kannalta, erityisesti jos “sisämallin” laskenta-alue on pieni.

Julkaisijayksikkö
Meteorologinen tutkimus

Luokitus (UDK)
551.509.313.43

Asiasanat
mesoskaalan numeerinen sääennustus, konvektio, mikrofysiikka, säteily

ISSN ja avainnimike
0782-6117 Finnish Meteorological Institute Contributions

ISBN
951-697-620-4 (paperback), 952-10-3613-3 (pdf)

Kieli
Englanti

Sivumäärä
136

Hinta

Myynti
Ilmatieteen laitos / Kirjasto
PL 503, 00101 Helsinki

Lisatietoja

This work is dedicated to *Matias* and *Katariina*

PREFACE

The work presented in this thesis has been carried out at the Department of Meteorology (later known as Division of Atmospheric Sciences) of the University of Helsinki and at the Numerical Weather Prediction (NWP) group at the Finnish Meteorologial Institute (FMI).

I want to express my gratitude to my supervisor Prof. Hannu Savijärvi of the University of Helsinki for support and help, especially in the beginning of my scientific career. I would also like to thank Hannu for his courage to employ me, although I was barely taken the first steps in the field of meteorology. Sincere thanks to Dr. Petri Räisänen, who helped and teached me a lot about the radiation processes in the atmosphere.

I wish to thank Prof. Mikko Alestalo, Deputy Director of FMI, for employing me at FMI to continue my work. I am truely thankful to Dr. Carl Fortelius, the head of NWP-group of FMI, who convinced Mikko that I should be hired. Furthermore, I would like to thank Carl and Dr. Juhani Damski, the head of meteorological research of FMI, for creating an inspireing working atmosphere and for their continuous encouragement and support in this process.

I would like to thank Prof. Sylvain Joffre of FMI and Prof. Rein Rõõm of University of Tartu for thier in-depth review of my thesis and for their valuable comments.

During the years I have been privileged to work with many great persons. Warm thanks to all the friends and colleagues at University of Helsinki and FMI (especially in the NWP-group) for all the enjoyable moments I have been sharing with you. Without your help and support, this thesis wouldn't have seen the daylight.

I would like to thank to my family and in-laws. Most importantly, I want to experess my deepest gratitude to my wife, Katariina, and to my son, Matias, for their love, support and all the dearest moments together. I owe you of having a real life. After all, this book in your hand is only work.

Helsinki, December 2006

Sami Niemelä

Contents

LIST OF ORIGINAL PUBLICATIONS

I Niemelä S., Räisänen P. and Savijärvi H., (2001): Comparison of surface radiative flux parameterizations Part I: Longwave radiation. *Atmos. Res.*, **58**, 1–18.

II Niemelä S., Räisänen P. and Savijärvi H., (2001): Comparison of surface radiative flux parameterizations Part II: Shortwave radiation. *Atmos. Res.*, **58**, 141–154.

III Savijärvi H., Niemelä S. and Tisler P., (2005): Coastal winds and low level jets: Simulations for sea gulfs. *Q. J. R. Meteorol. Soc.*, **131**, No. 606, 625–637.

IV Niemelä S. and Fortelius C., (2005): Applicability of large scale convection and condensation parameterization to meso-γ-scale HIRLAM: a case study of a convective event. *Mon. Wea. Rev.*, **133**, No. 8, 2422–2435.

V Tisler P., Gregow E., Niemelä S. and Savijärvi H., (2005): Wind field prediction in coastal zone: operational mesoscale model evaluation and simulations with increased horizontal resolution. *Journal of Coastal Research* (accepted).

1 INTRODUCTION

Modern-day weather forecasting is highly relying on Numerical Weather Prediction (NWP). Since the beginning of NWP at the end of 1940's (Charney and Eliassen, 1949), NWP-applications have always been among the first to fully utilise the ever-increasing computing power, by improving the model resolution and by removing various simplifying approximations from the mathematical set of equations. Present-day (2006) operational NWP has reached a level, where the models covering the whole globe have a horizontal resolution of about 20–40 km. On the other hand, Limited Area Models (LAM) operate with grid-sizes of about 10 km. Lately, in all the LAM communities, the trend has been to aim to scales of 1–4 km, the so-called meso-γ-scale after Orlanski (1975). Consequently, this *again* requires more computing power in order to fully utilise the potential behind high-resolution NWP-methods.

What more can we achieve from the improved computing capabilities by increasing the model resolution towards the meso-γ-scale? Several studies (e.g., Mass et al., 2002) have addressed this question and have come to the conclusion that a large positive impact on precipitation and wind forecasts can be reached by decreasing the grid-size from scales currently used in global NWP models to around 10 km. However, when going from scales of about 10 km to km-scale, it is harder to extract any additional value out from the NWP-systems. Statistical verification scores for heavy precipitation and wind structures near meso-scale orographic features (i.e. coastlines, mountains and valleys) are only marginally improved.

In a nutshell, the meso-γ-scale NWP-system should be able to help to predict extreme weather like severe convective phenomena with strong precipitation fallout. In principle, km-scale atmospheric models with highly sophisticated treatment of physical processes are able to simulate, even forecast, such meso-scale structures (e.g., Weisman et al. 1997; Mass et al. 2002; Tao et al. 2003). Therefore, the effort to develop a km-scale NWP-system with the additional computational cost is justified. We should not underestimate the potential damages due to extreme weather. Even in high-latitude regions like Finland (in between 60°N–70°N), severe mesoscale convective systems with physical and economical losses are common during summertime (Punkka and Bister, 2005).

However, models based on less approximated equations (e.g., nonhydrostatic, compressible, fully elastic) with the sophisticated treatment of physical processes is still computationally extremely expensive. How detailed systems do we really need in order to predict extreme weather events? Weather services lacking high computing power would especially benefit if a computationally more efficient 'intermediate' solutions could be found.

The objective of this thesis is to evaluate some physical parameterization methods used in high-resolution NWP-models. PAPER I covers the offline intercomparison of different longwave radiative flux parameterizations in extreme winter conditions,

whereas PAPER II concentrates on shortwave radiative flux parameterizations. PAPER IV studies convection and microphysics parameterizations in a 3-dimensional high-resolution NWP-model environment. In PAPER III and PAPER V, issues related to high-resolution marine wind prediction are considered. The aim in PAPERS III–V is to evaluate the applicability of the existing model physics when model resolution increases from about 10 km towards the km-scales.

2 PRINCIPLES OF THE NUMERICAL WEATHER PREDICTION

The actual NWP-system contains two main components: the atmospheric model and the data assimilation system. The model itself can be divided into two parts: the model dynamics and physical parameterizations. The following sections give a brief introduction to all of these components following the notation used in the books of Pielke (2002) and Holton (1992). Furthermore, the physical parameterization schemes more relevant to this thesis are described in a more detailed manner in Sections 3.1 and 3.2.

2.1 MODEL DYNAMICS

The core of the *model dynamics* is the set of hydrodynamic equations, which govern the state of the atmosphere. Any atmospheric model requires the following conservation equations (see e.g. Pielke, 2002)

$$\frac{\partial \rho}{\partial t} = -(\nabla \cdot \rho \bar{\mathbf{V}}) \tag{2.1}$$

$$\frac{\partial \bar{\mathbf{V}}}{\partial t} = -\bar{\mathbf{V}} \cdot \nabla \bar{\mathbf{V}} - \rho^{-1} \nabla p + \bar{\mathbf{g}} - 2\bar{\mathbf{\Omega}} \times \bar{\mathbf{V}} + \bar{\mathbf{F}}_{\mathbf{r}} \tag{2.2}$$

$$\frac{\partial \theta}{\partial t} = -\bar{\mathbf{V}} \cdot \nabla \theta + S_\theta \tag{2.3}$$

$$\frac{\partial q_n}{\partial t} = -\bar{\mathbf{V}} \cdot \nabla q_n + S_{q_n} \tag{2.4}$$

and

$$\frac{\partial \chi_m}{\partial t} = -\bar{\mathbf{V}} \cdot \nabla \chi_m + S_{\chi_m} \tag{2.5}$$

Eqs. (2.1)–(2.5) represent the conservation equations of mass, motion, heat, water (in solid, liquid and vapour forms) and any other gaseous (chemical) species in the atmosphere, respectively. In the above equations $\bar{\mathbf{V}} = u\bar{\mathbf{i}} + v\bar{\mathbf{j}} + w\bar{\mathbf{k}}$ represents the 3-dimensional wind vector, ρ is the air density, p is the pressure, $\bar{\mathbf{g}} = -g\bar{\mathbf{k}}$ is the gravity vector, $\bar{\mathbf{\Omega}}$ is the angular velocity of the earth, $\bar{\mathbf{F}}_{\mathbf{r}}$ is the friction force by the molecular process, θ is the potential temperature, q_n is the mass ratio between water (either solid, liquid or vapour) and air in the same volume, χ_m is the mass ratio between any chemical species and air in the same volume and t is the time. Finally, all the S-terms refer to sources and sinks of heat, water and chemical species.

The full set presented above contains several small terms, which are unimportant for NWP purposes. In current NWP applications the chemistry (Eq. 2.5) is almost completely excluded due to its small impact on large scale flow. The representation of the

source and sink term S_{χ_m} can be complex and, therefore, computationally expensive. The molecular processes (in Eq. 2.2) are also negligible on the resolvable scale.

Equation (2.1) states that the atmosphere is compressible and, therefore, the air density is a prognostic variable. Traditionally, in NWP-applications the $\frac{\partial \rho}{\partial t}$-term is considered to be so small that it can be neglected. Furthermore, Eq. (2.1) can be simplified by making either the *anelastic approximation*, whereby the density of the basic state is assumed to be horizontally homogenous, or even the more restrictive *incompressibility approximation*, with the assumption of constant basic state density. Another common simplification is the *hydrostatic approximation* in Eq. (2.2). In that case, the vertical acceleration term ($\frac{\partial w}{\partial t}$) is neglected. Consequently, the gravitational acceleration and the vertical pressure gradient force balance each other. This assumption is valid when the horizontal extent of the circulation is larger than its vertical counterpart.

Numerical methods are utilised to solve the above set of coupled partial differential equations. However, these conservation equations must be averaged over finite spatial and temporal scales due to limited computing power. Therefore, all the dependent variables (marked as ϕ) are divided as follows (Pielke, 2002):

$$\phi = \overline{\phi} + \phi^{'}$$

where $\overline{\phi}$ is a dependent variable averaged over a finite space (with grid lengths Δx, Δy, Δz) and time Δt, while $\phi^{'}$ represents the sub-grid variations around the averaged state. This averaging is applied to all variables in Eqs. (2.1)–(2.5). As a result, the averaged equations contain averaged terms (e.g., $\frac{\partial \overline{u}}{\partial t}$, $-\overline{\rho}^{-1}\nabla\overline{p}$), which can be resolved explicitly by the model dynamics. The size of the averaging volume determines the *model resolution*: the smaller the averaged space the higher the model resolution. Furthermore, the price of the averaging procedure is the appearance of sub-grid-scale correlation terms (e.g., $\overline{w^{'}\theta^{'}}$, $\overline{u^{'}w^{'}}$) in the averaged equations. These terms represent the net effect of small scale atmospheric phenomena onto the resolved scale state. However, sub-grid-scale correlation terms cannot be resolved explicitly but their net effect has to be estimated utilising *physical parameterization* methods.

2.2 PHYSICAL PARAMETERIZATIONS

The fundamental idea behind the physical parameterization procedure is to estimate the sub-grid-scale terms (e.g., S_θ, S_{q_n}, $\overline{w^{'}\theta^{'}}$) by using the averaged prognostic variables (e.g., $\overline{u}$, $\overline{v}$, $\overline{\theta}$). The complexity of the parameterization problem is mainly determined by model resolution. Some processes, like *radiation*, *cloud microphysics* and interactions between the atmosphere and the surface, are always needed in atmospheric models. They contribute to the averaged state through the source terms S_θ and S_{q_n}. However, it is still feasible to introduce some simplifications. For example, most of the current

NWP-models exclude the prognostic treatment of falling precipitation, some even exclude cloud water and ice (in Eq. 2.4 and S-terms). With the horizontal grid-scales (about 10 km or more) used by current NWP-models, the sub-grid correlation terms mainly represent the vertical fluxes of momentum, heat and moisture due to small *turbulent* eddies and larger *convective* secondary circulations. However, when approaching the km-scales, circulation patterns related to organised deep convection begin to be resolved by the averaged equations (Weisman et al., 1997). Consequently, the deep convection parameterization becomes unnecessary.

2.3 DATA ASSIMILATION

In principle, the model described in Sections 2.1 and 2.2 is able to simulate all the meteorologically important flow structures. This itself is not enough for producing a good forecast. The model integration is also critically dependent on the initial conditions. The procedure that links the initial state of the atmospheric model to reality is called *data assimilation*. State-of-the-art data assimilation systems are based on the 3-

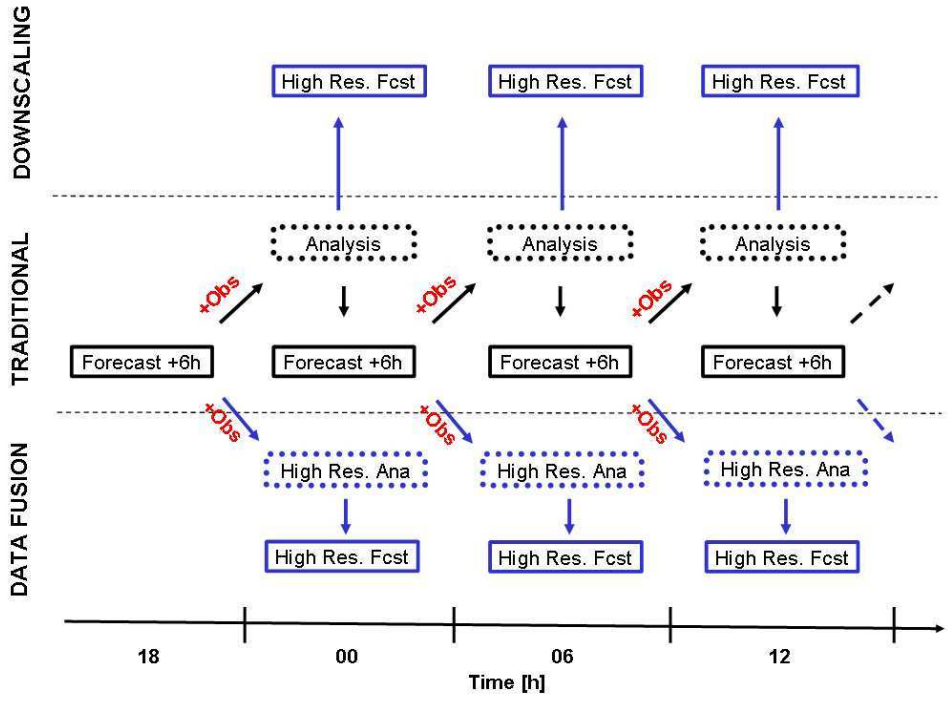

FIGURE 2.1. Data assimilation cycle. The black boxes represent the traditional data assimilation cycle. The blue boxes illustrate two alternative ways how to embed a km-scale model (downscaling method on the top and the data fusion technique at the bottom) inside a host model (the one with the full cycle). Dotted boxes represent the analysis phase, whereas solid boxes are the forecasts.

or 4-dimensional variational methods. The aim is to derive a model state (called an analysis), in which the differences with respect to observations and to a background state (usually a short-term forecast) are simultaneously minimised. Figure 2.1 shows a schematic graph of how the data assimilation cycle is traditionally organised. It also shows two common ways how to bring high-resolution information into a coarser resolution host model. The first method is the pure *downscaling*, where the analysis of the host model is interpolated to the high-resolution grid and used as it is. This approach allows the model to create itself a fine structure after some spin-up period. On the contrary, in the *data fusion* technique the high-resolution analysis is performed by using simple statistical methods on top of the coarser resolution background state (e.g., Albers et al., 1996). This method aims to reduce the spin-up time at the beginning of the model integration. The main difference between the data fusion and the traditional data assimilation is the role of observations. In the traditional way, observations 'correct' the large-scale structures and the fine-scale is taken from the background state. By contrast, in the data fusion method, the fine-scale structures are expected to be extracted from the observations. Therefore, the data fusion method highly relies on the existence of high-resolution observations, and especially on remote sensing data, i.e., satellites and radars.

3 PHYSICAL PARAMETERIZATIONS APPLIED IN NUMERICAL MODELS

In this thesis, the main tool for studying the effect of parameterization will be the High Resolution Limited Area Model (HIRLAM; Undén et al., 2002). HIRLAM is a complete NWP system including a hydrostatic primitive equation model with an extensive set of physical parameterizations and 3D variational data assimilation (3D-Var) system. In addition, a research version of the anelastic pressure-coordinate-based nonhydrostatic dynamics has been developed by Rõõm (2001) and Männik and Rõõm (2001). HIRLAM contains physical parameterization schemes for turbulence, convection and condensation, radiation and surface processes. The current turbulence scheme is based on the prognostic turbulent kinetic energy (TKE) and a diagnostic length scale l. This TKE-l scheme is adapted from the planetary boundary layer model of Cuxart et al. (2000). Soil and surface processes are modeled using the Interaction-Soil-Biosphere-Atmosphere (ISBA) scheme (Noilhan and Planton, 1989). In the current implementation, three land-surface types and two soil layers are available. Soil temperature and water content are simulated with the predictive force-restore methods. The fast radiation code is based on the work of Savijärvi (1990). Both the convective and stratiform condensation, clouds and precipitation are parameterized by the Soft TRansition COndensation (STRACO) scheme (Sass, 2002).

The main issues of this thesis are related to the parameterizations of radiation and convection-condensation. These processes are described in more details in sections 3.1 and 3.2, respectively.

3.1 RADIATIVE FLUX PARAMETERIZATION

The purpose of the radiation parameterization in an atmospheric model is to provide the surface radiative net fluxes and the atmospheric temperature tendencies at each grid point due to longwave (thermal LW, 4.0 μm–100 μm) and shortwave (solar SW, 0.3 μm–4.0 μm) radiation. This thesis concentrates on the surface fluxes, which can be observed and used for the validation of parameterization methods (PAPER I and PAPER II).

Downwelling LW and SW radiation fluxes are key terms of the surface energy budget in NWP-models and vitally important for many applications such as climate studies, agricultural meteorology (e.g., prediction of frost) and air-sea-ice interaction studies. Simplified equations for the longwave and shortwave downwelling fluxes at the surface can be described as

$$F_{\mathrm{LW}}^{\downarrow} = \varepsilon \sigma T_0^4 \tag{3.1}$$

and

$$F^{\downarrow}_{\mathrm{SW}} = \tau S \cos\Theta = \tau\psi S_{\mathrm{TOA}} \cos\Theta \tag{3.2}$$

In Eqs. (3.1)–(3.2), ε is the atmospheric emissivity, σ is the Stefan-Bolzmann constant, T_0 is the screen-level temperature, $S = \psi S_{\mathrm{TOA}}$ is the incident solar radiation at the top of the atmosphere on a surface perpendicular to the solar beam (S_{TOA} = 1367 Wm^{-2} is the solar constant and ψ accounts for the seasonal variations of the Earth-Sun distance), Θ is the solar zenith angle, and τ is a broadband atmospheric transmissivity.

In the LW part of the spectrum, the broadband atmospheric emissivity ε depends both on the vertical temperature profile and on the vertical distribution of radiatively active constituents; H_2O, CO_2 and clouds being the major contributors, O_3, CH_4, N_2O and the CFCs having a smaller role. In the case of SW-radiation, the solar elevation has a very strong effect on the downwelling flux at the surface. Factors contributing to atmospheric attenuation of solar radiation include gaseous absorption (most importantly, by H_2O and O_3), Rayleigh scattering by air molecules, and scattering and absorption by cloud droplets, ice crystals and aerosols.

Due to the nature of ε (see PAPER I), the near-surface temperature and humidity profiles are of primary importance in determining $F^{\downarrow}_{\mathrm{LW}}$. In addition, τ is strongly dependent on Θ (see PAPER II). For those reasons, it is tempting to try to approximate the clear-sky fluxes by only using the screen-level variables. In that case, the parameterization problem reduces formally to the representation of ε and τ as a function of screen-level vapour pressure e_0 and temperature T_0. Many such simple empirical methods have been proposed since Ångström (1918).

This thesis includes intercomparisons of both simple methods and more complex radiation parameterization schemes used in NWP-models: the scheme used earlier at ECMWF (European Centre for Medium-Range Weather Forecast) (Morcrette, 1991, hereafter EC-OLD), the DWD (Deutscher Wetterdienst; Ritter and Geleyn, 1992) scheme and the HIRLAM (Savijärvi, 1990) scheme. LW calculations are also performed with the RRTM (Rapid Radiative Transfer Model; Mlawer et al., 1997) scheme, which is currently in use at ECMWF. The comparison concentrates mainly on clear-sky conditions at the Jokioinen (60°49′ N, 23°30′ E) and Sodankylä (67°22′ N, 26°39′ E) observatories in Finland. However, the effects of clouds on surface fluxes are studied by using the simple 'correction schemes'. Hence, the clear-sky flux is multiplied by a cloud correction factor, which depends on the total cloudiness (see PAPER I and PAPER II).

3.2 CONVECTION AND CONDENSATION PARAMETERIZATION

The current convection and condensation parameterization of HIRLAM (STRACO-scheme) parameterizes both convective and stratiform condensation, clouds and precipitation processes. It also allows a gradual transition between both modes. The actual transition is handled by relaxing the fractional cloud cover towards an equilibrium, in

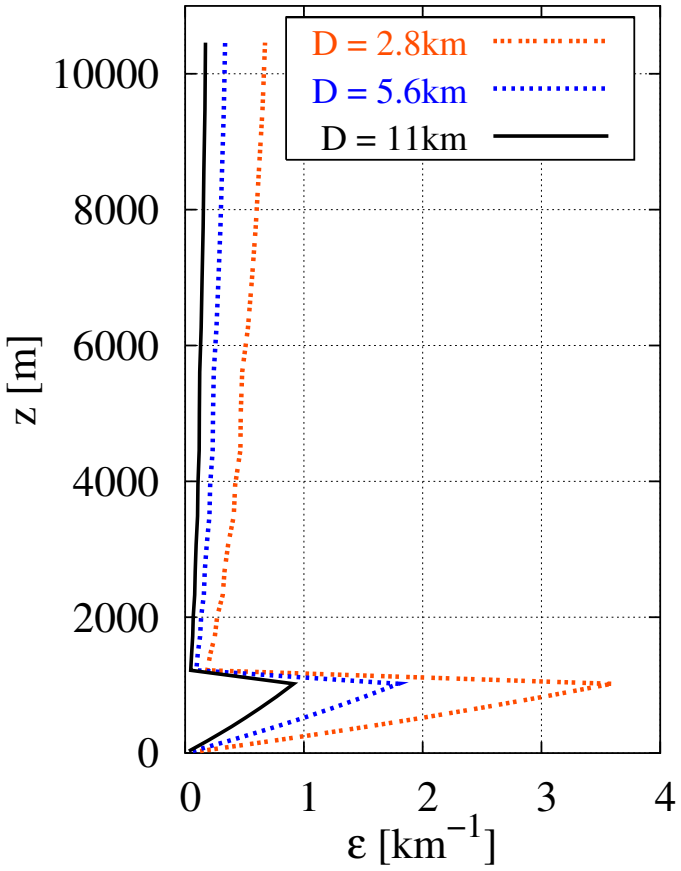

FIGURE 3.1. Entrainment ϵ profiles with variable grid sizes (2.8, 5.6 and 11 km) as described in PAPER IV by Eqs. (5)–(6). A fixed vertical wind shear of $|\frac{\partial V}{\partial z}| = 0.005$ s^{-1} is assumed. The lowest 1000 m is assumed to be dry adiabatic, whereas above the potential temperature profile is $|\frac{\partial \theta}{\partial z}| = 0.004$ Km^{-1}

which the cloud may be either in the convective or stratiform mode. STRACO was originally developed for the meso-β scales. However, an improved applicability for meso-γ scales is sought by introducing simple grid-size-dependent functions in the convective part of the scheme.

The STRACO scheme acts on the temperature T, specific humidity q and combined cloud water and ice content q_c (PAPER IV Eqs. 7–9). It also uses the horizontal wind components u and v and the surface pressure p_s. The scheme follows closely the work of Sundqvist et al. (1989) and Sundqvist (1993). The convective part is based on a moisture accession closure, as does the well-known Kuo (1974) scheme. However, the STRACO scheme differs considerably from the original Kuo scheme. The present version of the cumulus parameterization does not directly produce any precipitation. Moreover, the scheme increases q_c, which is a grid-scale prognostic variable.

The precipitation release depends diagnostically on q_c and is based on the formu-

lation of Sundqvist et al. (1989)

$$G_p = \Phi(\omega_*) q_c \left(1 - \exp(-\frac{q_c}{b\mu(\omega_*, B)}) \right) \tag{3.3}$$

In Eq. (3.3), $\Phi(\omega_*)^{-1}$ is a characteristic time for the conversion of cloud drops to rain drops, which depends on the model-resolved vertical velocity ω_*. The quantity $\mu(\omega_*, B)$ is the threshold value for cloud water, which depends on both vertical velocity and buoyancy B. Finally, b is the fractional cloud cover.

This thesis will address the grid-size-dependency of the present convection-condensation scheme. This grid-size-dependency is introduced in two components of the parameterization scheme: in the triggering phase and in the moistening parameter (PAPER IV Eqs. 15 and 16). The purpose of the moistening parameter is to define how much of the additional large-scale moisture input is consumed in the convective cloud condensation (and heating) process. Consequently, this also affects the formation of precipitation.

The triggering mechanism for convection defines the convective air columns by lifting the air layers. In HIRLAM, a convectively active air column is generated if the lifted air layer experiences positive buoyancy. This lifting method depends on the horizontal grid size in two ways. At first, resolution-dependent perturbation temperature and specific humidity are used at the beginning of the lifting process in order to simulate the energy source, which is needed to overcome the convective inhibition (PAPER IV, Eqs. 1–2). In this case, lifted air parcel reaches the level of free convection easier as grid size increases.

Secondly, the cloudy air is mixed with cooler ambient air during the air parcel ascent by using a grid-size-dependent entrainment profile (Fig. 3.1). This profile follows the work of Cohen (2000), which suggested that maximum entrainment is obtained near the cloud base. Figure 3.1 displays that lateral mixing will restrict the formation of convective entities by decreasing the buoyancy as the grid size reduces. Consequently, the convection parameterization is gradually switched off by restricting the depth of the convective cloud (see Eqs. 7–9 and 14 in PAPER IV).

4 MAIN RESULTS

In the following sections, the main results of the papers included in this thesis are discussed. Sections 4.1 and 4.2 cover PAPERS I and II, respectively. Section 4.3 concentrates on PAPER IV, whereas PAPERS III and V are reviewed in Section 4.4.

4.1 LONGWAVE RADIATION

The first finding in PAPER I is that all the included radiative flux schemes underestimate the clear-sky downwelling LW flux $F^{\downarrow}_{\mathrm{LW,clr}}$ at the surface (Table 4.1). This feature is more prominent in the empirical schemes and especially during wintertime. In general, the underestimation is smaller in the more detailed NWP-schemes. Naturally, the explanation is that NWP-schemes receive the temperature and moisture profiles as input, and, therefore the wintertime inversion is taken into account more properly. On the contrary, for empirical schemes such conditions remain out of reach.

The observed effective emissivity $\varepsilon_{\mathrm{eff}} = F^{\downarrow}_{\mathrm{LW,clr}}/\sigma T_0^4$ of the clear atmosphere is shown in Fig. 4.1 as a function of screen-level water vapour pressure e_0. The lowest values of $\varepsilon_{\mathrm{eff}}$ are obtained when the the vapour pressure is about 2 hPa. The higher values of $\varepsilon_{\mathrm{eff}}$ in dry (and very cold) screen-level conditions are explained by the prevailing strong inversions. These data suggest that a new empirical LW parameterization of the

Table 4.1 Results of the LW comparison in cloudless situations. The average measured LW flux values were 262 Wm^{-2} for summer 1997, 191 Wm^{-2} for winter 1997 and 162 Wm^{-2} for winter 1999.

	Summer 1997			Winter 1997			Winter 1999		
Schemes	Bias	SD	RMS	Bias	SD	RMS	Bias	SD	RMS
Ångström (1918)	-0.1	8.7	8.7	-18.2	16.0	24.3	-32.0	9.2	33.3
Brunt (1932)	-24.9	8.5	26.3	-40.5	14.4	42.9	-51.9	8.3	52.5
Swinbank (1963)	-16.8	8.9	19.0	-34.8	19.1	39.7	-52.9	12.1	54.3
Brutsaert (1975)	-11.1	9.1	14.3	-42.6	20.7	47.4	-64.3	14.2	65.9
Idso (1981)	9.2	8.5	12.6	-8.3	15.6	17.7	-22.7	9.1	24.5
Prata (1996)	-5.0	8.4	9.8	-17.5	14.6	22.8	-30.1	8.2	31.2
Dilley and O'Brien (1998)	-7.1	8.7	11.2	-19.4	13.7	23.8	-30.1	8.3	31.2
EC-OLD	-5.3	5.5	7.7	-22.9	8.3	24.3	-21.7	7.9	23.1
DWD	-14.8	5.0	15.6	-27.6	7.8	28.7	-26.9	7.8	28.0
HIRLAM	-7.0	5.7	9.0	-24.6	8.3	26.0	-24.3	8.0	25.6
RRTM	-1.5	5.1	5.3	-15.4	8.2	17.4	-14.3	8.4	16.6

Bias (Wm^{-2}) = parameterized−measured.
SD (Wm^{-2}) = standard deviation.
RMS (Wm^{-2}) = root-mean-square difference.

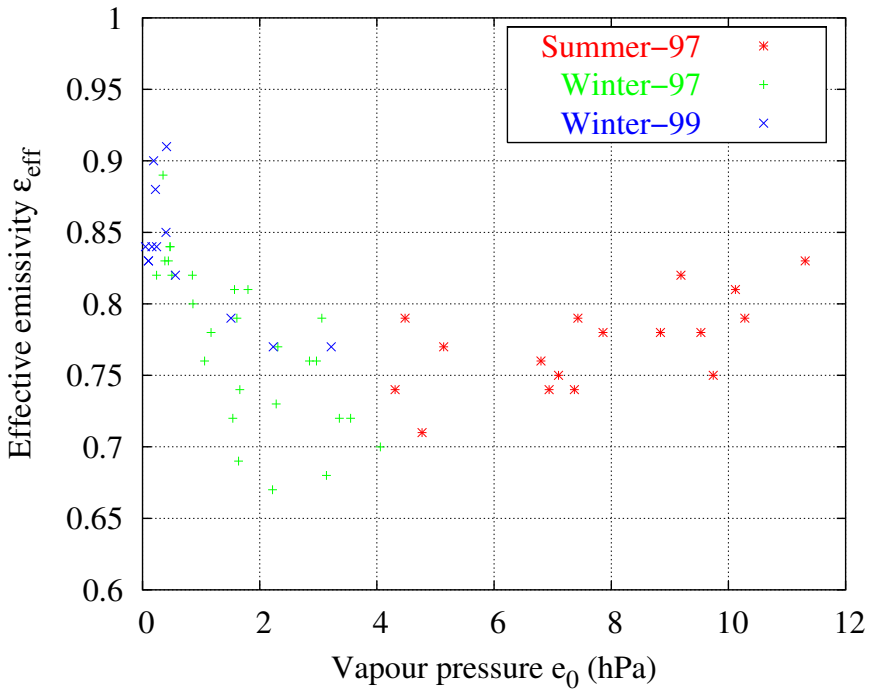

FIGURE 4.1. The 'observed' clear-sky effective emissivity ($\varepsilon_{\text{eff}} = F^{\downarrow}_{\text{LW,clr}}/\sigma T_0^4$) of the atmosphere in Sodankylä as a function of water vapour pressure (Fig. 3b in PAPER I).

form:

$$F^{\downarrow}_{\text{LW,clr}} = \begin{cases} (0.72 + 0.009[e_0 - 2])\sigma T_0^4 & \text{if } e_0 \geq 2, \\ (0.72 - 0.076[e_0 - 2])\sigma T_0^4 & \text{if } e_0 < 2 \end{cases} \tag{4.1}$$

could be employed. Results from applying Eq. (4.1) to Sodankylä data are better than for any other scheme, which uses screen-level input values only. The improvement is significant especially in cold and dry conditions. The bias and standard deviation in summer 1997, winter 1997 and winter 1999 are (−0.4/8.3), (−0.2/9.5) and (−3.2/7.1) [Wm^{-2}], respectively (cf. Table 4.1). Naturally, the performance is expected to be worse in climatic conditions significantly different from Sodankylä. However, it is believed that the general behavior seen in Fig. 4.1 is typical for all high-latitude continental stations, where surface inversions are common in clear-sky winter conditions (see e.g. Dutton, 1993; Walden et al., 1998).

The performance of the 'cloud correction' methods is studied by using the existing simple schemes of Jacobs (1978) and Maykut and Church (1973) for summertime conditions. In addition, we developed an alternative new all-sky flux parameterization using radiation and SYNOP-data from Sodankylä, summer 1997. The new scheme is based on the net all-sky flux scheme of Budyko (1974) and has the form

$$F^{\downarrow}_{\text{LW,all}} = \left(\ 1 + [\frac{F^{\uparrow}_{\text{LW,s}}}{F^{\downarrow}_{\text{LW,clr}}} - 1] \cdot 0.87 c^{3.49} \ \right) \ F^{\downarrow}_{\text{LW,clr}} \tag{4.2}$$

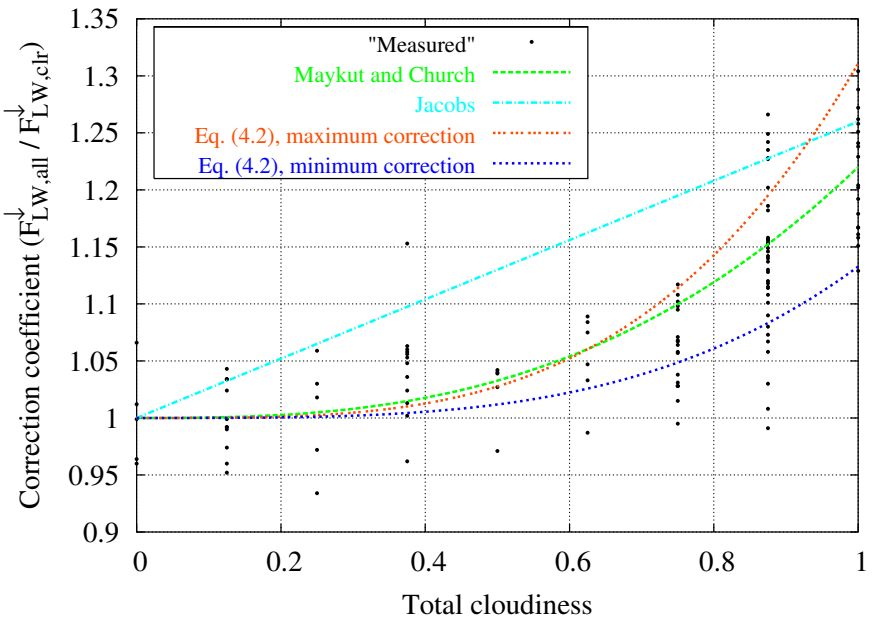

FIGURE 4.2. Longwave cloud correction coefficient ($F^{\downarrow}_{\mathrm{LW,all}}/F^{\downarrow}_{\mathrm{LW,clr}}$) as a function of total cloudiness (Fig. 5 in PAPER I). The dots represent the measured $F^{\downarrow}_{\mathrm{LW,all}}$ divided by the calculated clear-sky flux $F^{\downarrow}_{\mathrm{LW,clr}}$ (Eq. 4.1). The lines show the different all-sky schemes. The maximum and minimum correction lines are both related to the new scheme (Eq. 4.2). They correspond to the largest (1.356) and smallest (1.152) value of the ratio $F^{\uparrow}_{\mathrm{LW,s}}/F^{\downarrow}_{\mathrm{LW,clr}}$ in the present data set (Sodankylä, summer 1997).

where c is total cloudiness (in tenths). $F^{\uparrow}_{\mathrm{LW,s}}$ is the LW radiation flux emitted by the surface, and it can be calculated using the Stefan–Boltzmann law σT_{s}^4 if the surface temperature T_{s} is known.

The use of simple 'cloud correction' schemes for calculating the downwelling LW flux in cloudy conditions provides useful results for many applications. The new scheme (Eq. 4.2) gives the best results in all respects (cf. PAPER I, Table 2). Figure 4.2 shows the comparison of the cloud corrections together with observations as a function of total cloudiness. Here, the different nature of the schemes unfolds: Jacobs's (1978) linear scheme clearly overestimates the all-sky fluxes, whereas the scheme of Maykut and Church (1973) captures the curvy shape of the observations. Moreover, the new scheme brings some flexibility in the curvy shape and, consequently, more accurate results. The flexibility of Eq. (4.2) originates from the ratio $\frac{F^{\uparrow}_{\mathrm{LW,s}}}{F^{\downarrow}_{\mathrm{LW,clr}}}$, which indirectly (via T_{s}) takes into account the different effect of strongly emitting low clouds (large ratio) and weakly emitting high clouds (small ratio).

4.2 SHORTWAVE RADIATION

In the case of clear-sky SW radiation, the empirical scheme of Iqbal (1983) outperforms even the NWP-schemes, especially with Jokioinen data (Table 4.2). The results from Iqbal's scheme are considerably better than those from the other schemes, which only use screen-level variables. It should be borne in mind that the Iqbal's scheme used here is tuned to conditions prevailing in Jokioinen. Although the tuning improves the results, it does not play the decisive role. Standard deviation in the results of the HIRLAM and DWD schemes is similar, whereas results with the EC-OLD scheme contain more scatter. Furthermore, the HIRLAM scheme seems to be more 'transparent' for clear-sky SW radiation compared to other NWP-schemes. This behaviour could be due to the simpler formulation of the HIRLAM-scheme, in which the SW part of the spectrum is treated using a single broadband interval. On the contrary, in the EC-OLD and DWD schemes, the SW spectrum is divided into two and three intervals, respectively.

The accuracy of the SW 'cloud correction' schemes is generally poor (PAPER II, Table 2). Figure 4.3 shows both the 'observed' and parameterized SW cloud correction coefficients. As for the LW radiation, the linear dependence of Berliand (1960) does not represent the observed structure. However, the curved shape of the Laevastu's (1960) scheme follows the measured trend. A major problem with the cloud corrections is the uncertainty in cloud optical properties, the optical thickness being the most important one. Therefore, an alternative new parameterization (hereafter 'low cloud

Table 4.2 Results of the SW comparison in cloudless situations. The average measured SW flux values were 378 Wm^{-2} for Jokioinen and 356 Wm^{-2} for Sodankylä.

	Jokioinen 1997			Sodankylä 1997		
Schemes	Bias	SD	RMS	Bias	SD	RMS
Paltridge and Platt (1976)	-16.1	29.7	33.8	-41.1	21.5	46.4
Moritz (1978)	-13.8	42.7	44.8	-38.1	30.3	48.7
Bennett (1982)	-5.2	20.7	21.3	-26.2	26.1	37.0
Zillman (1972)	11.7	37.0	38.8	-15.4	27.5	31.5
Shine (1984)	15.7	23.4	28.2	-10.5	17.8	20.7
Iqbal (1983)	-1.1	12.4	12.4	-19.9	8.3	21.5
EC-OLD	5.9	19.7	20.6	-16.3	14.1	21.5
DWD	2.9	13.7	14.0	-17.2	8.0	19.0
HIRLAM	13.6	13.1	18.9	-6.0	9.9	11.5

Bias (Wm^{-2}) = parameterized−measured.
SD (Wm^{-2}) = standard deviation.
RMS (Wm^{-2}) = root-mean-square difference.

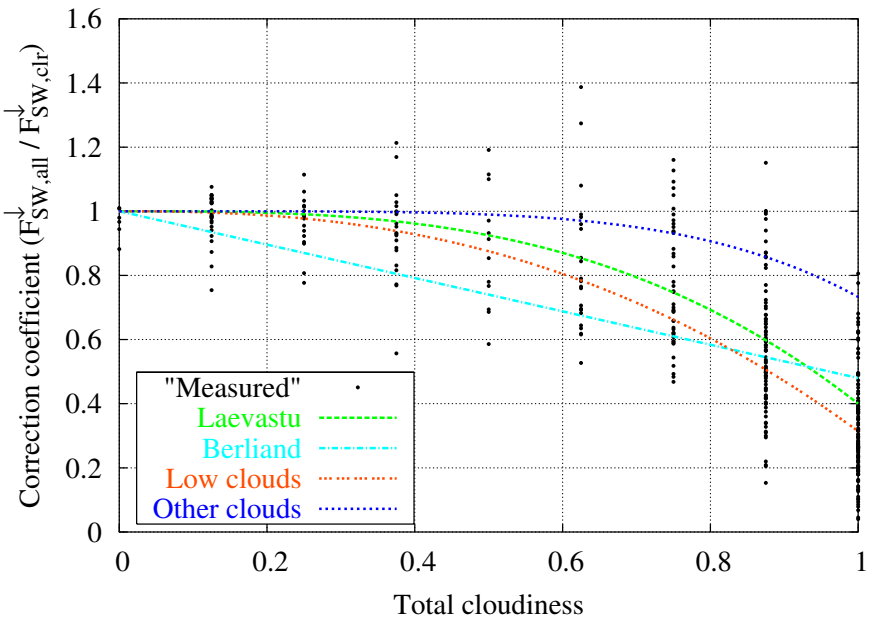

FIGURE 4.3. Shortwave cloud correction coefficient ($F^{\downarrow}_{\mathrm{SW,all}}/F^{\downarrow}_{\mathrm{SW,clr}}$) as a function of total cloudiness. The dots represent the measured $F^{\downarrow}_{\mathrm{SW,all}}$ divided by the calculated clear-sky flux $F^{\downarrow}_{\mathrm{SW,clr}}$ (Iqbal, 1983). The lines are for the referred all-sky schemes. The lines 'low clouds' and 'other clouds' are both related to the 'low cloud scheme': the former gives the correction in cases in which the whole visible cloud cover consists of low clouds, while the latter represents cases with middle and/or high clouds only (Fig. 4 in PAPER II).

scheme') is derived using radiation and cloudiness data from Jokioinen, Finland, 1997, where the amounts of low, middle and high clouds are available separately (from synop observations).

$$F^{\downarrow}_{\mathrm{SW,all}} = (1 - c^{[4.7-2.24\cdot\frac{c_{\mathrm{low}}}{c+10^{-3}}]} + 0.31c_{\mathrm{low}}^{2.46} + 0.73c_{\mathrm{oth}}^{4.7})F^{\downarrow}_{\mathrm{SW,clr}} \tag{4.3}$$

where c is total cloudiness, c_{low} is the amount of low clouds and c_{oth} ($= c - c_{\mathrm{low}}$) is the amount of 'other clouds'. The low cloud scheme accounts implicitly for the fact that low clouds tend to be optically thicker than higher clouds. Overall, the best results are obtained with the new scheme, although the improvement is only marginal (PAPER II, Table 2).

4.3 CONVECTION AND PRECIPITATION

The performance of the HIRLAM convection and condensation scheme is evaluated for three horizontal grid-sizes: 11, 5.6 and 2.8 km. The main emphasis is to assess the importance of the grid-size-dependent features of the current scheme. Model results are

Table 4.3 Summary of the experiment runs.

		GSD* in the convection scheme	
Name	Dynamics	Triggering	Moistening parameter
HH-1	Hydrostatic	yes	yes
NHH-1	Nonhydrostatic	yes	yes
NHH-2	Nonhydrostatic	yes	no
NHH-3	Nonhydrostatic	no	no

* GSD = grid-size dependency

compared to observed radar reflectivity data utilising a Radar Simulation Model (PAPER IV, Section 2c), which calculates radar reflectivities from the three-dimensional model output.

Table 4.3 summarises 4 basic experiments, which were conducted with variable model configurations. The comparison between NHH-1 and NHH-2 focuses on the choice of the moistening parameter (see explanation in Section 3.2). The issue of the grid-size-dependent triggering procedure was studied by comparing NHH-2 and NHH-3. The differences in the performance of hydrostatic and nonhydrostatic models can be studied by comparing the experiments HH-1 and NHH-1.

Figure 4.4 shows the radar reflectivity (proportional to rain intensity) frequency distributions produced by different model configurations. All configurations tend to overestimate the areas of both very strong (>32 dBZ) and very weak (<8 dBZ) reflectivity. Although the overestimation of weak echoes is in most of the cases noticeable, the focus should be on the strong echoes, because of their larger practical importance.

The best reflectivity distribution is obtained with a fully grid-size dependent convection scheme (NHH-1) and with a 5.6 km grid-spacing. None of the convection schemes employed with a 2.8 km grid spacing were able to produce satisfactory results. In that case, the current configuration of convection parameterization combined with diagnostic precipitation parameterization seems to overestimate the amount of very strong reflectivities. Diagnostic representation of precipitation processes cannot explicitly account for the drag effect caused by the weight of falling precipitation. The drag effect can be an important factor, which suppresses the upward vertical motions in a numerical model (e.g., Kato and Saito, 1995) and, concequently, leads to smaller precipitation amount. Although this effect is crudely parameterized in Eq (3.3) using a model-resolved vertical velocity, it seems, however, to be too ineffective.

Figure 4.5 presents 12-hour accumulated areal precipitation as a function of grid size. Figs. 4.5 b and c show how the total precipitation is composed of a stratiform and convective part. NHH-1 produces average precipitation amount that are close to the

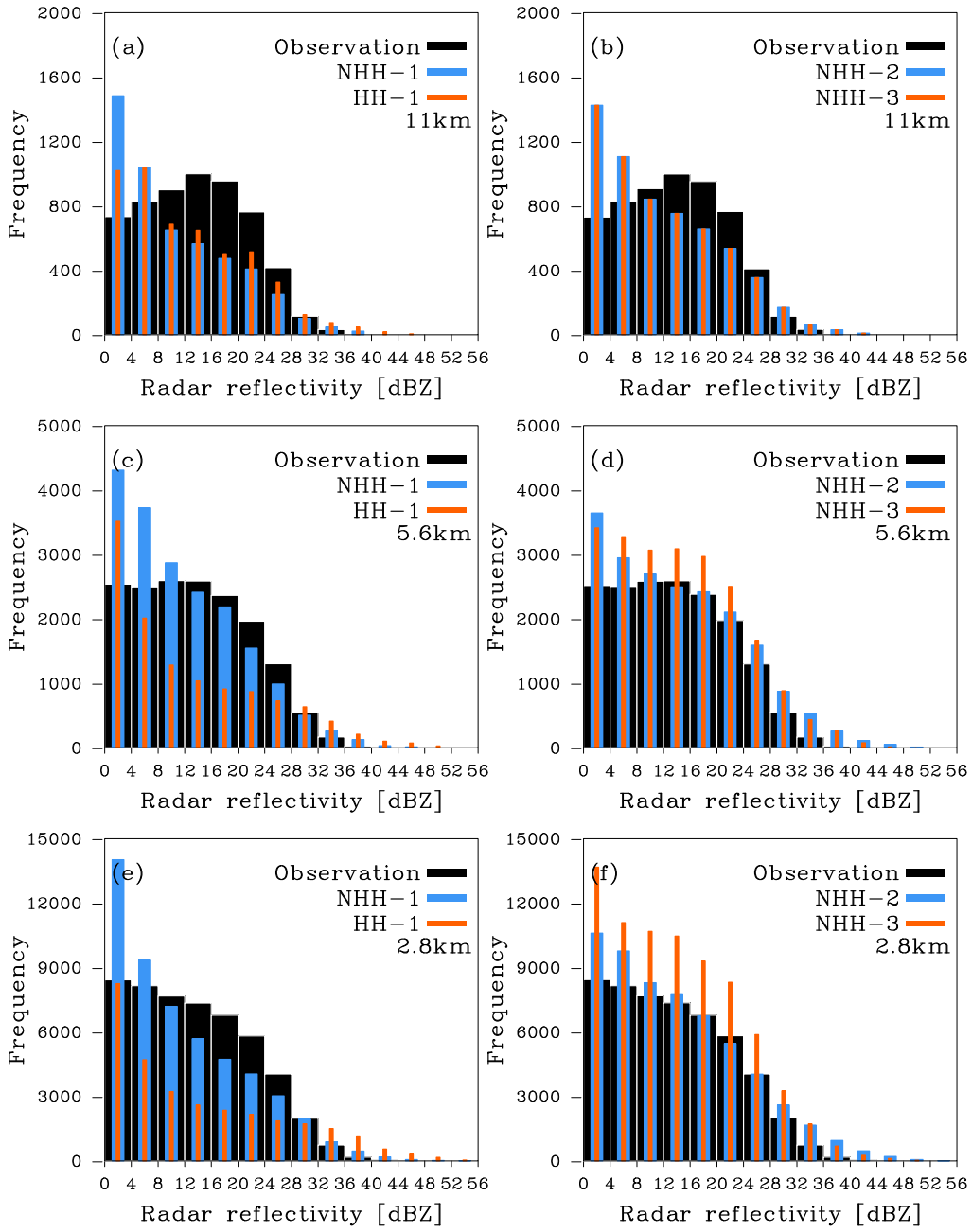

FIGURE 4.4. Frequency distributions of radar reflectivity [dBZ] produced by 21 hour simulations starting at 00 UTC 25 May 2001. In (a), (c) and (e) the distributions are from NHH-1 and HH-1. In (b), (d) and (f) the distributions are from NHH-2 and NHH-3. Black bars represent dBZ-observations. Rows from top to bottom present horizontal grid spacings of 11, 5.6 and 2.8 km, respectively. The radar antenna elevation is 0.4°. In this case reflectivity values below 0 dBZ are not meteorologically important and are therefore omitted (Figs. 2 and 3 in PAPER IV).

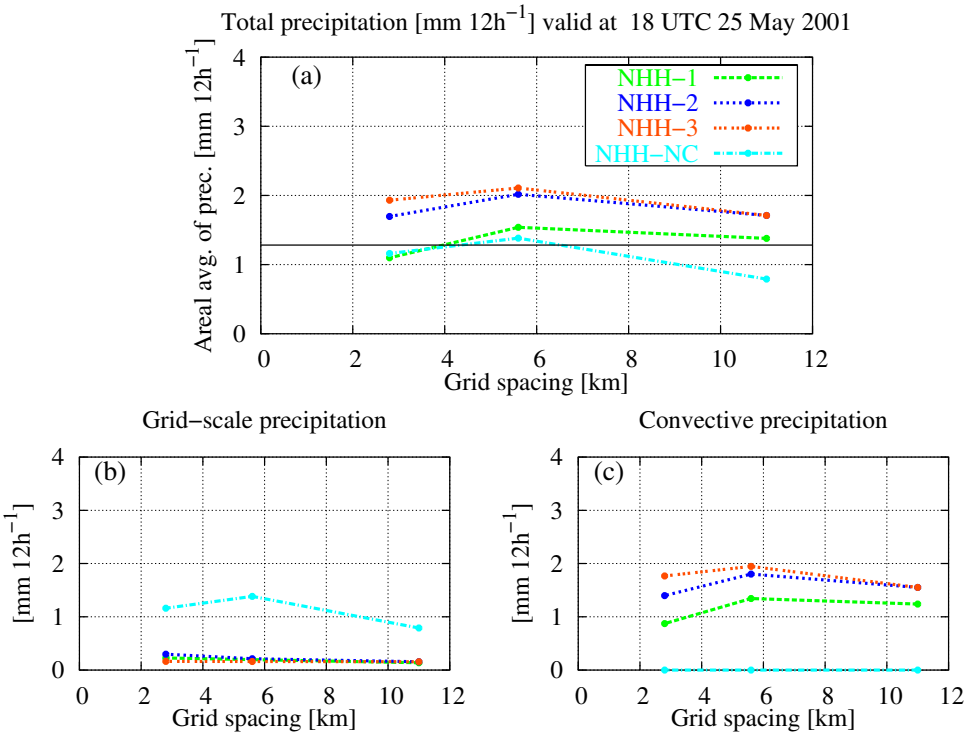

FIGURE 4.5. Areally-averaged 12-hour accumulated precipitation as a function of the grid spacing. (a) Total precipitation, (b) grid-scale precipitation and (c) convective precipitation. Areal averages are defined over the area shown in PAPER IV, Fig. 1. The solid horizontal line in graph (a) represents an areally-averaged radar retrieval of accumulated precipitation provided by the Baltex Radar Data Centre (Fig. 5 in PAPER IV).

observed value provided by the Baltex Radar Data Centre (Koistinen and Michelson, 2002). The schemes using non-grid-size-dependent moistening parameter (Eq. 15 in PAPER IV) overestimate the areal precipitation at all grid spacings. This moistening parameter depends on vertically averaged relative humidity within the convective entity. In moist conditions, as presented here, the majority of additional moisture source is consumed by the convective heating and condensation processes. Concequently, an increased amount of cloud condensate leads to enhanced precipitation release.

The grid-size-dependent triggering mechanism for convection (difference between NHH-2 and NHH-3) decreases the overestimation of the areal averaged precipitation (NHH-2, in Fig. 4.5) by reducing the frequency of moderate radar reflectivies (Figs. 4.4 b, d and f). However, the grid-size-dependency does not compensate the overall overestimation of the strong reflectivities. One hypothesis to explain such a behaviour is a feedback mechanism related to the accumulation of instability. The triggering of the convection scheme becomes more ineffective due to increased model resolution. Consequently, convective instability is able to slowly build up in the model. This leads to stronger resolved-scale updraft and low level convergence. The convergence drives moisture into the area of convectively unstable air. Eventually, when the convection scheme is activated, it has now more moisture to be consumed in heating and conden-

sation processes. Furthermore, this again leads to more intense rainfall. However, this hypothesis has not been confirmed in this study.

In this case, the model with the nonhydrostatic dynamics (NHH-1) outperforms the one with the hydrostatic approximation (HH-1) at the 5.6 and 2.8 km grid sizes (Figs. 4.4 a, c and e). With an 11 km grid spacing, the behaviour of both models is very similar. The hydrostatic model tends to create too strong reflectivities at the expense of weaker ones when operating with a dense grid.

4.4 WIND

PAPER III explores the reasons for the formation of relatively strong coastal afternoon surface winds along the Gulf of Finland under typical summertime conditions. Based on the experience of forecasters, the near surface winds tend to be relatively strong, even supergeostrophic, when the wind direction is along the coast. It is also noticed that such a behaviour is not captured by the large-scale NWP-models.

According to the idealised two-dimensional meso-scale model of the University of Helsinki, the reason for the strong coastal winds is the inertial oscillation mechanism, when the large-scale flow is from the south-east or from the west. In that case, the location and geometry of the Gulf is favorable for an inertial oscillation yielding a low

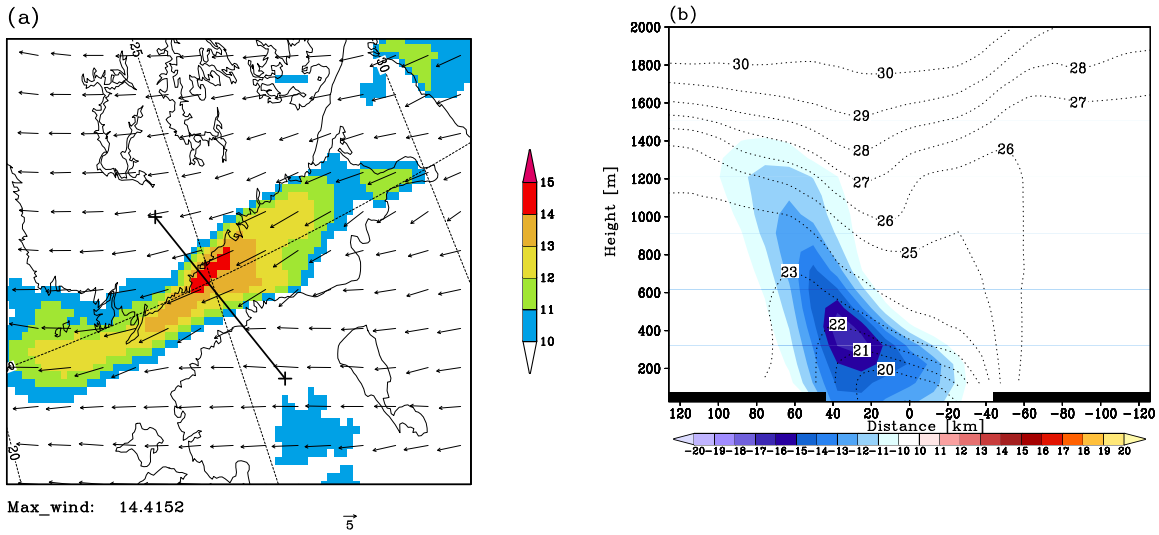

FIGURE 4.6. HIRLAM +12 h wind forecast valid on 29 August 1997, 12 UTC. (a) Wind vectors and wind velocity (m s^{-1}) at the lowest model level (about 30 m). (b) Cross sections (Finland on the left and Estonia on the right, along the line in a) of the HIRLAM potential temperature (lines, °C) and wind component parallel with the coastline (colors, m s^{-1}). The negative values are towards the viewer and only the values $|v| > 9$ m s^{-1} are shown for clarity (Figs. 8 and 9 in PAPER III).

level jet (LLJ) near the Finnish coast due to reduced turbulent friction over the sea. This feature is further enhanced by the sea-breeze circulation (PAPER III, Fig. 3 and 4). A high model resolution is needed to catch these phenomena.

A case-study is conducted for 29 August 1997, where the three-dimensional hydrostatic HIRLAM model with a 7.7 km grid size is employed. The aim of the test is to study whether the findings from the 2D-model are valid also in the 3D-environment. The selected case closely corresponds to the idealised 2D-experiments; geostrophic wind (about 10 ms^{-1}) blowing roughly from the south-east and a cloudless sky.

Figure 4.6a shows the wind speed and direction at the lowest model level after 12 h model integration. Figure 4.6b illustrates the corresponding cross-section of the potential temperature and wind speed parallel to the coastline. The wind speed in HIRLAM is very close to the observed values (PAPER III, Fig. 7). Moreover, with this 7.7 km grid size, HIRLAM is able to form a LLJ next to the Finnish coast similarly to the 2D-experiments. A sea breeze circulation is also resolved by HIRLAM in this clear-sky case.

PAPER V presents wind verifications based on forecasts of two operational HIRLAM models and high-resolution experiments (with HIRLAM and MM5). In the HIRLAM experiments, the improved model resolution alone, without touching the physical parameterizations, does not necessary improve the wind forecasts. Other factors, e.g., turbulence parameterization and the quality of the host model, are also important to the high-resolution modeling of the wind speed and direction.

5 DISCUSSION

All LAM communities are aiming to increase the resolution of operational NWP systems towards scales of 1–4 km. However, there are still practical and scientific questions concerning the configuration of NWP-models operating with such a high resolution. To what extent the current model physics is applicable when approaching km-scales? What is required from the model physics at meso-γ scales? When does the hydrostatic assumption lose its validity? The aim of this study is to gain knowledge on high resolution NWP and partly clarify these issues.

The validity of the hydrostatic assumption depends on the studied case. The hydrostatic model dynamics is applicable with a km-scale grid size when modelling atmospheric phenomena, which are vertically shallow compared to their horizontal extent, like the LLJ presented in PAPER III. On the other hand, flow structures related to strong vertical accelerations (e.g., moist convection and orographically forced updrafts) are nonhydrostatic by nature. PAPER IV shows that in a single moist convective case the nonhydrostatic dynamics of the HIRLAM-model was beneficial compared to hydrostatic dynamics when a grid size was reduced below 5.6 km. Therefore, it is recommended that nonhydrostatic model dynamics should be used in NWP applications with a grid size smaller than 5 km in so far as it is computationally feasible.

One of the challenging issue facing km-scale NWP modelling is the representation of convection. When convective flow structures become resolvable? Weisman et al. (1997) showed that flow structures related to an organised deep convection could be resolved explicitly (without convection parameterization) using a km-scale model. However, Bryan et al. (2003) argued that a model resolution of about 1–4 km is not enough for capturing in-cloud flow structures, although the general structure of the cumulonimbus cloud may be well represented. If no convection parameterization is used, models may end up to a situation, where the convective updrafts are forced to develop within too large grid volume. This will lead to slowly evolving and overshooting precipitation events. For this reason, it may turn out that some parameterization is still needed (especially for shallow convection) with km-scale model resolutions. One simple solution could be a grid-size-dependent deep convection parameterization scheme, in which the efficiency of the scheme is reduced with increasing model resolution. PAPER IV showed that the convection scheme of the HIRLAM-model has a potential to be assigned for such a task. However, instead of using deep convection parameterization a more sophisticated approach could be an integrated scheme for boundary layer turbulence and clouds.

While the resolution of NWP models is approaching scales where it is possible to explicitly resolve organised convective systems, at the same time the cloud microphysics parameterization will have a more significant role. It is important to properly take into account the detailed representation of the different water phases and their effect on meso-scale flow patterns. This requires the prognostic treatment of cloud wa-

ter, cloud ice, rain, snow, graupel and even hail (e.g., Tao et al., 2003). It should be emphasised that the microphysical parameterization of the HIRLAM-model (presented in PAPER IV) does not fulfil these requirements (prognostic treatment only for cloud condensate).

What is the role of the radiation parameterization in a high resolution NWP-system? As the microphysical parameterization becomes all the more detailed, the requirements for the radiation parameterization become more demanding. The radiation scheme should be able to take into account the detailed representation of the different prognostic hydrometeors. In some cases, radiation processes may even be important for short-term cloud formation/dissipation at the meso-scale. One practical problem is that with current computing facilities, running a highly detailed radiation scheme (like RRTM presented in PAPER I) is computationally expensive. Therefore, in some km-scale NWP applications, the radiation scheme is activated, e.g., only every 15 minutes. Since the life cycle of a convective cloud is about 30–40 minutes (e.g, Emanuel, 1994), the use of coarse update intervals for radiation processes is questionable. Although the radiation parameterization of the HIRLAM-model is computationally fast, it is less accurate compared to more detailed schemes (PAPER I and PAPER II). Thus, it would be interesting to study which aspect is more important at the meso-scale, the accuracy or the efficiency of the radiation parameterization. This was left for future studies.

6 CONCLUSIONS

The present thesis concentrates on assessing some key physical parameterization methods used in NWP-models. One of the main issues was the evaluation of the grid-size-dependent convection and condensation parameterization in a high-resolution meso-scale model (grid size less than 10 km). Furthermore, meso-scale models were utilised in wind prediction studies near coastlines. This thesis also includes intercomparisons of several radiative-flux parameterization schemes.

As shown in PAPER I and PAPER II, the clear-sky LW flux is calculated more accurately by the NWP-schemes than by simpler schemes. Naturally, the main reason for that is the use of the temperature and water vapour profiles as input values instead of screen values only. As mentioned in PAPER I, the most important emission source of the clear-sky LW radiation in the atmosphere is water vapour close to the surface. By contrast, for the clear-sky SW flux, the simple methods can still compete with the NWP-schemes. Under extreme winter conditions, even the more sophisticated NWP-parameterizations seem to be too 'transparent' for both LW and SW clear-sky radiation.

Simple cloud correction functions are useful in predicting the LW radiative flux in cloudy conditions. However, the feasibility of the cloud correction methods is questionable in the SW part of the spectrum. The most important cloud properties affecting LW and SW radiation are cloud base temperature (proportional to height) and cloud optical thickness, respectively. The total cloudiness observation alone is not adequate for providing the cloud depth information.

All the empirical radiative flux parameterizations are more or less site specific and case dependent, especially the new ones introduced in this thesis. For example, the night-time inversions might be overpresented in the present data set. Therefore, in the future it is recommended to test the new schemes under climatic conditions significantly different from those prevailing in Finland.

PAPER IV studies the performance of the grid-size-dependent convection scheme when the grid size of a NWP model is decreased towards the km-scales. The resolution dependent triggering function for convection is clearly beneficial for the high resolution models. It decreases the overestimation of the precipitation by cutting down the frequency of moderate rain intensities. Furthermore, the grid-size-dependent moistening parameter reduces the overprediction even more by restricting convective condensation. However, this formulation is highly simplified and too case-dependent for providing a satisfactory solution for all scales. Overall, the present convection and condensation scheme of HIRLAM is still applicable with a 5.6 km grid size. On the other hand, with a 2.8 km grid spacing, this scheme seems to be still too active (too intense rainfall), although, it tries to switch the convection parameterization off due to grid-size-dependency.

The issues related to the prediction of the marine wind in the vicinity of the coastline are considered in PAPER III and PAPER V. It is shown that the HIRLAM model

with a 7.7 km grid size, hydrostatic dynamics and current operational physical parameterizations, is able to produce the a LLJ over the Gulf of Finland in a similar way as the 2D model experiments and the observations suggest. However, the increased model resolution itself does not necessarily improve the wind forecasts, as seen in PAPER V. In nested systems where a fine-scale model is embedded inside a large-scale NWP model, the quality of the forecast produced by the forcing host model is really important. Especially when the fine-scale domain is small, the possible false information from the host model spreads rapidly into the inner domain and contaminates the high-resolution results.

In general, the verification of high-resolution models is very difficult using data only from a single station. For the wind, the location of the grid square with respect to the coastal observation site starts to play too important role, especially in areas of highly complex land-sea distribution. Therefore, the use of high-resolution remote sensing data for verification should be further studied.

In this study, the performance of the high-resolution NWP models has been assessed only in individual cases. Future studies should be extended to a larger variety of atmospheric phenomena. More attention should be directed in particular to severe weather situations (e.g., thunderstorms with extreme precipitation and strong winds). In addition, the version of the HIRLAM convection and condensation scheme tested here should be validated in parallel with more sophisticated microphysical schemes that have prognostic variables for different hydrometeors and explicit convection. Another interesting topic is to test further the validity of the hydrostatic approximation under different atmospheric conditions with a variable grid size.

SUMMARIES OF THE ORIGINAL PUBLICATIONS

I Niemelä S., Räisänen P. and Savijärvi H., (2001): Comparison of surface radiative flux parameterizations Part I: Longwave radiation. *Atmos. Res.*, **58**, 1–18.

PAPER I presents a comparison of several longwave downwelling radiative flux parameterizations with hourly averaged pointwise surface radiation observations made at Sodankylä, Finland, in 1997 and 1999. Both clear and cloudy night-time conditions were considered. The clear-sky comparisons included eight simple LW parameterizations, which mainly use screen level input data, and four radiation schemes from NWP-models. For the cases with clouds, three simple cloud correction methods were tested. The author was responsible for all the analyses and for a major part of the calculations and writing.

II Niemelä S., Räisänen P. and Savijärvi H., (2001): Comparison of surface radiative flux parameterizations Part II: Shortwave radiation. *Atmos. Res.*, **58**, 141–154.

In PAPER II, a comparison of several shortwave downwelling radiative flux parameterizations in Jokioinen and Sodankylä, Finland, is presented. Both clear and cloudy conditions were considered. The clear-sky comparisons included six simple SW parameterizations, which use screen level input data, and three radiation schemes from NWP-models. For the cases with clouds, three simple cloud correction methods were tested. The author was responsible for all the analyses and for a major part of the calculations and writing.

III Savijärvi H., Niemelä S. and Tisler P., (2005): Coastal winds and low level jets: Simulations for sea gulfs. *Q. J. R. Meteorol. Soc.*, **131**, No. 606, 625–637.

PAPER III explored the reasons for the relatively strong coastal afternoon winds observed along the Gulf of Finland. This phenomenon was mainly studied by using a high-resolution 2D numerical model with variable geostrophic wind speed and direction. The effects of sea breeze were investigated by modifying the cloud cover in the model. In addition, a case study was made with a three-dimensional operational NWP-model to test the findings from 2D-experiments. The author's contribution was to carry out the NWP-model runs and analyse their results. He was also partly responsible for writing about the 3D case study.

IV Niemelä S. and Fortelius C., (2005): Applicability of large scale convection and condensation parameterization to meso-γ-scale HIRLAM: a case study of a convective event. *Mon. Wea. Rev.*, **133**, No. 8, 2422–2435.

PAPER IV presents a case study of a single cold air outbreak event with widespread convective precipitation over Southern Finland on 25 May 2001. The purpose of the study was to investigate the applicability of the convection and condensation scheme of the HIRLAM model at meso-γ scales. The study concentrated on the

issue of grid-size-dependent convection parameterization. At the same time, the performance of an experimental nonhydrostatic version of HIRLAM was evaluated. Model simulations were conducted with three different horizontal grid spacings: 11, 5.6 and 2.8 km. Model results were compared to observed radar reflectivity data utilising a Radar Simulation Model, which calculates radar reflectivities from three-dimensional model output. The author was responsible for all the NWP-modeling and for a major part of the analyses and writing.

V Tisler P., Gregow E., Niemelä S. and Savijärvi H., (2005): Wind field prediction in coastal zone: operational mesoscale model evaluation and simulations with increased horizontal resolution. *Journal of Coastal Research* (accepted).

PAPER V discusses the comparison of two different versions of the operational HIRLAM model in order to verify wind forecasts on the eastern coast of Gulf of Bothnia against good-quality single observations (an island station and a station at the coastline). In addition, two cases were studied in more detail using also the Penn State/NCAR Mesoscale Model (MM5) and a nonhydrostatic version of HIRLAM. The detailed simulations were carried out with three different horizontal resolutions. The author's contribution was rather minor in providing the model data of nonhydrostatic HIRLAM simulations to the study.

REFERENCES

Albers, S. C., J. A. McGinley, D. L. Brikenheuer, and J. R. Smart, 1996: The local analysis and prediction system (LAPS): analyses of clouds, precipitation, and temperature. *Wea. Forecasting*, **11**, 273–287.

Bennett, T. J., 1982: A coupled atmosphere-sea ice model study of the role of sea ice in climatic predictability. *J. Atmos. Sci.*, **39**, 1456–1465.

Berliand, T. C., 1960: Method of climatological estimation of global radiation. *Meteorol. Gidrol.*, **6**, 9–12.

Brunt, D., 1932: Notes on radiation in the atmosphere. *Q. J. R. Meteorol. Soc.*, **58**, 389–420.

Brutsaert, W., 1975: On a derivable formula for long-wave radiation from clear skies. *Water Resour. Res.*, **11**, 742–744.

Bryan, G. H., J. C. Wyngaard, and J. M. Fritsch, 2003: Resolution requirements for the simulation of deep moist convection. *Mon. Wea. Rev.*, **131**, 2394–2416.

Budyko, M. I., 1974: *Climate and life*. Academic Press, New York.

Charney, J. G. and A. Eliassen, 1949: A numerical method for predicting the perturbations of the middle latitude westerlies. *Tellus*, **1**, 38–54.

Cohen, C., 2000: A quantitative investigation of entrainment and detrainment in numerically simulated cumulonimbus clouds. *J. Atmos. Sci*, **57**, 1657–1674.

Cuxart, J., P. Bougeault, and J.-L. Redelsperger, 2000: A turbulence scheme allowing for mesoscale and large-eddy simulations. *Q. J. R. Meteorol. Soc.*, **126**, 1–30.

Dilley, A. C. and D. M. O'Brien, 1998: Estimating downward clear sky long-wave irradiance at the surface from screen temperature and precipitable water. *Q. J. R. Meteorol. Soc.*, **124**, 1391–1401.

Dutton, E. G., 1993: An extended comparison between LOWTRAN7 computed and observed broadband thermal irradiances: global extreme and intermediate surface conditions. *J. Atmos. Ocean. Technol.*, **10**, 326–336.

Emanuel, K. A., 1994: *Atmospheric Convection*. Oxford University Press, New York.

Holton, J. R., 1992: *An introduction in dynamic meteorology*. Academic Press, San Diego, California.

Idso, S. B., 1981: A set of equations for full spectrum and 8- to 14-μm and 10.5- to 12.5-μm thermal radiation from cloudless skies. *Water Resour. Res.*, **17**, 295–304.

Iqbal, M., 1983: *An introduction to solar radiation*. Academic Press, 390 pp.

Jacobs, J. D., 1978: Radiation climate of Broughton Island. Energy budget studies in relation to fast-ice breakup processes in Davis Strait. *Occas. Pap.*, **26**, 105–120, inst. of Arctic and Alp. Res., University of Colorado, Boulder, United States.

Kato, T. and K. Saito, 1995: Hydrostatic and non-hydrostatic simulations of moist convection: applicability of the hydrostatic approximation to a high-resolution model. *J. Meteor. Soc. Japan*, **73**, 59–77.

Koistinen, J. and D. B. Michelson, 2002: Baltex weather radar-based products and their accuracies. *Boreal. Env. Res.*, **7**, 253–263.

Kuo, H. L., 1974: Further studies of parameterization of the influence of cumulus convection on large-scale flow. *J. Atmos. Sci.*, **31**, 1232–1240.

Laevastu, T., 1960: Factors affecting the temperature of the surface layer of the sea. *Commentat. Phys.-Math.*, **25**.

Männik, A. and R. Rõõm, 2001: Nonhydrostatic adiabatic kernel for HIRLAM. Part II: Anelastic, hybrid-coordinate, explicit-Eulerian model. HIRLAM Tech. Rep. 49, SMHI, S-601 76 Norrköping, Sweden, Hirlam-5 Project, 51 pp. [available online at http://hirlam.org/open/publications/TechReports/].

Mass, C. F., D. Ovens, K. Westrick, and B. A. Colle, 2002: Does increasing horizontal resolution produce more skillful forecasts? *Bull. Am. Meteor. Soc.*, **83**, 407–430.

Maykut, G. A. and P. F. Church, 1973: Radiation climate of Barrow, Alaska, 1962–66. *J. Appl. Meteor.*, **12**, 620–628.

Mlawer, E. J., S. J. Taubman, P. D. Brown, M. J. Iacono, and S. A. Clough, 1997: Radiative transfer for inhomogenous atmospheres: RRTM, a validated correlated-k model for the longwave. *J. Geophys. Res.*, **102 (D14)**, 16663–16682.

Morcrette, J.-J., 1991: Radiation and cloud radiative properties in the European Centre for Medium Range Weather Forecasts forecasting system. *J. Geophys. Res.*, **96 (D5)**, 9121–9132.

Moritz, R. E., 1978: A model for estimating global solar radiation. Energy budget studies in relation to fast-ice breakup processes in Davis Strait. *Occas. Pap.*, **26**, 121–142, inst. of Arctic and Alp. Res., University of Colorado, Boulder, United States.

Noilhan, J. and S. Planton, 1989: A simple parameterization of land surface processes for meteorological models. *Mon. Wea. Rev.*, **117**, 536–549.

Orlanski, I., 1975: A rational subdivision of scales for atmospheric processes. *Bull. Amer. Met. Soc.*, **56**, 527–530.

Paltridge, G. W. and C. M. R. Platt, 1976: *Radiative processes in meteorology and climatology*. Elsevier, Amsterdam, 318 pp.

Pielke, R. A., 2002: *Mesoscale meteorological modeling*. Academic Press, New York, 2nd edition.

Prata, A. J., 1996: A new long-wave formula for estimating downward clear-sky radiation at the surface. *Q. J. R. Meteorol. Soc.*, **122**, 1127–1151.

Punkka, A.-J. and M. Bister, 2005: Occurrence of summertime convective precipitation and mesoscale convective systems in Finland during 2000–01. *Mon. Wea. Rev.*, **133**, 362–373.

Rõõm, R., 2001: Nonhydrostatic adiabatic kernel for HIRLAM. Part I: Fundamentals of nonhydrostatic dynamics in pressure-related coordinates. HIRLAM Tech. Rep. 48, SMHI, S-601 76 Norrköping, Sweden, Hirlam-5 Project, 25 pp. [available online at http://hirlam.org/open/publications/TechReports/].

Ritter, B. and J.-F. Geleyn, 1992: A comprehensive radiation scheme for numerical weather prediction models with potential applications in climate simulations. *Mon. Wea. Rev.*, **120**, 303–325.

Sass, B. H., 2002: A research version of the STRACO cloud scheme. DMI Tech. Rep. 02-10, Danish Meteorological Institute, DK-2001 Copenhagen, Denmark, 25 pp. [available online at http://www.dmi.dk/dmi/index/viden/dmi-publikationer/tekniskerapporter.htm].

Savijärvi, H., 1990: Fast radiation parameterization schemes for mesoscale and short-range forecast models. *J. Appl. Meteor.*, **29**, 437–447.

Shine, K. P., 1984: Parametrization of the shortwave flux over high albedo surfaces as a function of cloud thickness and surface albedo. *Q. J. R. Meteorol. Soc.*, **110**, 747–764.

Sundqvist, H., 1993: Inclusion of ice phase of hydrometeors in cloud parameterization for mesoscale and largescale models. *Contrib. Atmos. Phys.*, **66**, 137–147.

Sundqvist, H., E. Berge, and J. E. Kristjánsson, 1989: Condensation and cloud parameterization studies with a mesoscale numerical weather prediction model. *Mon. Wea. Rev.*, **117**, 1641–1657.

Swinbank, W. C., 1963: Long-wave radiation from clear skies. *Q. J. R. Meteorol. Soc.*, **89**, 339–348.

Tao, W.-K., D. Starr, A. Hou, P. Newman, and Y. Sud, 2003: A cumulus parameterization workshop. *Bull. Amer. Met. Soc.*, **84**, 1055–1062.

Ångström, A., 1918: A study of the radiation of the atmosphere. *Smithson. Misc. Collect.*, **65**, 1–159.

Undén, P., L. Rontu, H. Järvinen, and Coauthors, 2002: *HIRLAM-5 Scientific Documentation*. HIRLAM-5 project, c/o Per Undén SMHI, S-601 76 Norrköping, Sweden, 144 pp. [available online at http://hirlam.org/open/publications/SciDoc_Dec2002.pdf].

Walden, V. P., S. G. Warren, and F. J. Murcray, 1998: Measurements of the downward longwave radiation spectrum over the Antarctic Plateau and comparisons with a line-by-line radiative transfer model for clear skies. *J. Geophys. Res.*, **103 (D4)**, 3825–3846.

Weisman, M. L., W. C. Skamarock, and J. B. Klemp, 1997: The resolution dependence of explicitly modeled convective systems. *Mon. Wea. Rev.*, **125**, 527–548.

Zillman, J. W., 1972: A study of some aspects of the radiation and heat budgets of the southern hemisphere oceans. *Meteorological Study*, **26**, Bur. of Meteorol., Dep. of the Inter., Canberra, Australia.